

University of Nebraska - Lincoln DigitalCommons@University of Nebraska - Lincoln

Ralph Skomski Publications

Research Papers in Physics and Astronomy

2015

Spin-modified catalysis

R Choudhary

University of Nebraska-Lincoln, Indian Institute of Technology Mandi

Priyanka Manchanda

University of Nebraska-Lincoln, priyanka.manchanda@vanderbilt.edu

Axel Enders

University of Nebraska-Lincoln, a.enders@me.com

Balamurugan Balamurugan

University of Nebraska-Lincoln, balamurugan@unl.edu

Arti Kashyap

Indian Institute of Technology Mandi, akashyap@lnmiit.ac.in

See next page for additional authors

Follow this and additional works at: <http://digitalcommons.unl.edu/physicsskomski>

 Part of the [Physics Commons](http://digitalcommons.unl.edu/physicscommons)

Choudhary, R; Manchanda, Priyanka; Enders, Axel; Balamurugan, Balamurugan; Kashyap, Arti; Sellmyer, David J.; and Skomski, Ralph A., "Spin-modified catalysis" (2015). *Ralph Skomski Publications*. 93.
<http://digitalcommons.unl.edu/physicsskomski/93>

This Article is brought to you for free and open access by the Research Papers in Physics and Astronomy at DigitalCommons@University of Nebraska - Lincoln. It has been accepted for inclusion in Ralph Skomski Publications by an authorized administrator of DigitalCommons@University of Nebraska - Lincoln.

Authors

R Choudhary, Priyanka Manchanda, Axel Enders, Balamurugan Balamurugan, Arti Kashyap, David J. Sellmyer, and Ralph A. Skomski

Spin-modified catalysis

R. Choudhary,^{1,2} P. Manchanda,¹ A. Enders,¹ B. Balamurugan,¹ A. Kashyap,²
 D. J. Sellmyer,¹ E. C. H. Sykes,³ and R. Skomski^{1,a)}

¹Department of Physics and Astronomy and NCMN, University of Nebraska, Lincoln, Nebraska 68588, USA

²School of Basic Sciences, Indian Institute of Technology Mandi, Mandi 175001, Himachal Pradesh, India

³Department of Chemistry, Pearson Chemistry Laboratory, Tufts University, Medford, Massachusetts 02155, USA

(Presented 7 November 2014; received 24 September 2014; accepted 4 December 2014; published online 15 April 2015)

First-principle calculations are used to explore the use of magnetic degrees of freedom in catalysis. We use the Vienna *Ab-Initio* Simulation Package to investigate both L1₀-ordered FePt and CoPt bulk materials and perform supercell calculations for FePt nanoclusters containing 43 atoms. As the catalytic activity of transition-metal elements and alloys involves individual d levels, magnetic alloying strongly affects the catalytic performance, because it leads to shifts in the local densities of states and to additional peaks due to magnetic-moment formation. The peak shift persists in nanoparticles but is surface-site specific and therefore depends on cluster size. Our research indicates that small modifications in stoichiometry and cluster size are a useful tool in the search for new catalysts. © 2015 AIP Publishing LLC. [<http://dx.doi.org/10.1063/1.4917328>]

I. INTRODUCTION

The principle of catalysis infers that a substance or nanostructure participates in a chemical reaction but does not enter the reaction products, remaining in its original form after the reaction. In other words, catalysis does not affect chemical equilibrium but facilitates the reaction by reducing energy barriers that kinetically inhibit the reaction.¹ While some reactions, such as ammonia synthesis and Fischer-Tropsch processes, are performed over Fe and/or Co, the purpose of this paper is to explore possibilities and mechanisms for using *magnetic degrees of freedom* in chemical catalysis. Emphasizing chemical catalysis is important to distinguish the present research from magnetic catalysis in quantum-field theory, which refers to symmetry breaking caused by a magnetic field.²

Our focus is on the quantum mechanics of catalysis using magnetic nanoparticles, a topic of potential importance in hydrogenation and hydrogen production.^{3,4} Such clusters can be fabricated by several methods such as cluster deposition.⁵ Magnetic nanoparticles play an important role in catalysis, but they normally act as substrates or "supports" for catalytically active substances and to move or separate catalysts with the help of magnetic fields.^{3,6–8} Nanoparticles also provide a favorable large surface-to-volume ratio,⁴ as exemplified by Pd:Pt core-shell nanoparticles⁶ for the hydrogenation of methyl acrylate. Sometimes, nanoparticles are directly involved in catalysis, for example, FePt and CoPt for acetylene to ethylene hydrogenation³ and spinel ferrites in microwave-assisted oxidation catalysts.⁹ Note that Pt and Pd are of great importance in catalysis and alloys, such as FePt and CoPt, are also chemically quite stable.

Catalysis requires a precise control of the electron energy levels of the catalyst, to ensure that the involved quantum-mechanical hybridization processes facilitate the desired chemical reaction.¹ For this reason, catalysts often contain transition metals, where the five d orbitals per atom create complicated densities of states (DOS), with many peaks caused by different atomic lattice planes. These peaks are well-understood quantum-mechanically¹⁰ and reproduced by density-functional theory, both in general and in the context of catalysis.^{11–15} The same strategy is behind our magnetic approach, except that the spin splitting yields additional levels to work with. While the envisaged chemical reactions are nonmagnetic in nature, magnetism provides an additional degree of freedom to fine-tune the DOS landscape.

II. THEORETICAL METHODS

To study L1₀ bulk magnets and the FePt nanoclusters, we have used the Vienna *ab initio* Simulation Package (VASP). A generalized-gradient approximation (GGA) is chosen for the exchange-correlation functional¹⁶ and a plane-wave basis using the projector augmented wave method set describes the valence electrons.¹⁷ The lattice parameters for the L1₀-ordered FePt are $a = b = 3.86 \text{ \AA}$ and $c = 3.729 \text{ \AA}$,¹⁸ and a gamma-centered k -point mesh is used for the calculations.

To ensure well-defined k -states, we have performed supercell calculations where the particles are periodically repeated in space. The particles have a surface-to-surface spacing of 5 \AA to ensure that the tails of the atomic wave functions do not introduce a hybridization error by hybridization through the vacuum. Furthermore, a small artificial line broadening is used in the calculations to accelerate convergence. No relaxation has been performed for the clusters,

^{a)}Author to whom correspondence should be addressed. Electronic mail: rskomski@unl.edu.

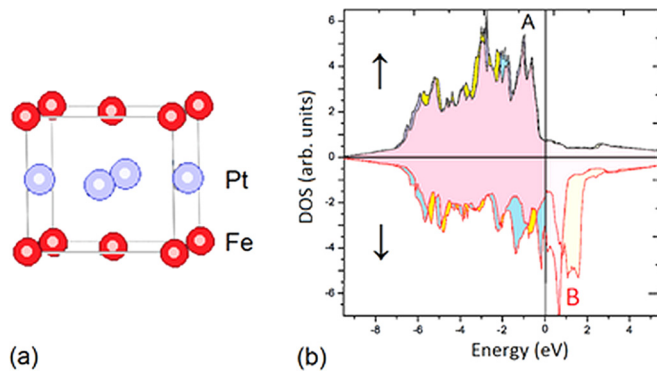


FIG. 1. Bulk $L1_0$ -ordered FePt and CoPt: (a) structure of FePt and (b) densities of state for $L1_0$ -ordered FePt (yellow/pink) and CoPt (blue/pink).

so that the peak positions in the local density of states contain some error.

III. RESULTS

A. Bulk FePt and CoPt

Figure 1 shows the $L1_0$ structure and the DOS for bulk FePt and CoPt. Figure 1(b) illustrates how the substitution of Co for Fe changes the bulk DOS when going from FePt (yellow) to CoPt (blue). The majority (\uparrow) band is fully occupied and "pinned" relative to the Fermi level (region A in the figure), whereas the position of the minority band (\downarrow) is changed by the Co (region B). A well-known feature of some alloys is solid solubility, that is, the stoichiometry is not fixed but can take arbitrary values. The system $Fe_{1-x}Co_xPt$ is a typical example. Due to the solid solubility between FePt and CoPt, the shift of the DOS peaks is a continuous function of the Co concentration, which makes it possible to fine-tune the energy levels that enable the catalytic reaction.

B. Nanocluster geometry and basic electronic structure

Figure 2(a) shows the atomic structures of our FePt clusters, which contain 43 atoms. The average diameter of the cluster is about 7.5 Å. Figure 2(b) divides the atomic position into crystallographically equivalent sites. There are altogether 7 seven nonequivalent sites, 2 Fe sites (I–II), and 5 Pt sites (III–VII).

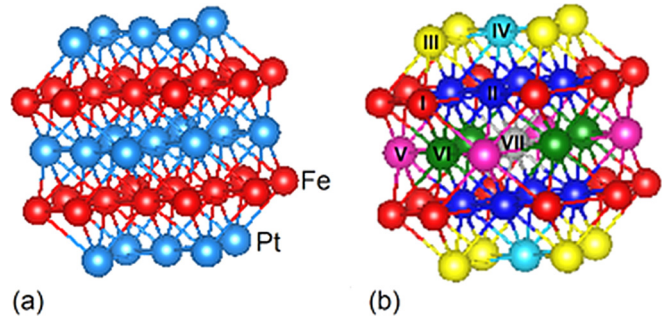


FIG. 2. FePt nanoparticle containing 43 atoms: (a) structure and (b) nonequivalent sites.

Figure 3(a) shows the total d density of states, which is an average over all atomic positions. The difference between the DOS of bulk $L1_0$ FePt and of FePt clusters is caused by the atoms on the cluster surface. This well-understood phenomenon¹⁹ is important for catalysis, because atoms in the center of a cluster cannot contribute to the catalytic reaction but can change the surface atom's DOS by ligand or strain effects.

The corresponding quantum-mechanical concept is the *local* density of states, obtained by projecting the total DOS onto atomic orbitals $\phi_{i\mu}(\mathbf{r}) = \phi_{\mu}(\mathbf{r} - \mathbf{R}_i)$, where μ is an orbital index. The starting point for the determination of the local DOS is the wave function $\psi_{\mathbf{k}\nu}(\mathbf{r})$, as obtained from the electronic-structure calculation, where ν is a band index that also includes spin. Projecting the total wave functions onto the atomic orbitals, $\langle \psi_{\mathbf{k}\nu} | \phi_{i\mu} \rangle$, yields the local density of states¹⁰

$$D_{i\mu}(E) = \sum_{\nu} \int_{\mathbf{k}} \delta(E - E_{\mathbf{k}}) \langle \psi_{\mathbf{k}\nu} | \phi_{i\mu} \rangle \langle \phi_{i\mu} | \psi_{\mathbf{k}\nu} \rangle d\mathbf{k}. \quad (1)$$

When the distinction between different orbitals μ , for example, between $|\text{Fe}(4s)\rangle$ and $|\text{Fe}(3d_{xy})\rangle$, is of secondary importance then it is sufficient to consider $D_i(E) = \sum_{\mu} D_{i\mu}(E)$. Figure 3(b) illustrates the difference between total and local DOS by showing the local DOS for the "gray" Pt atom in the center of the cluster. The most striking feature is the absence of the minima in the spin-down DOS above the Fermi level, as expected for Pt.

Note that both nanoparticles and bulk alloys contain sharp peaks, in the latter case caused by crystalline lattice planes. Due to reduced coordination, the DOS gets somewhat narrower at surfaces,¹⁰ but the main effect is the potentially

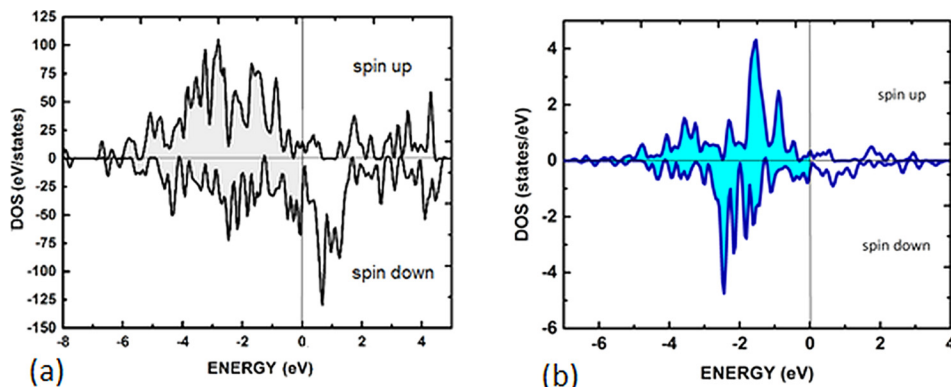


FIG. 3. Typical DOS for the FePt nanoparticle of Fig. 2: (a) total DOS and (b) local DOS for the central atom (site VII).

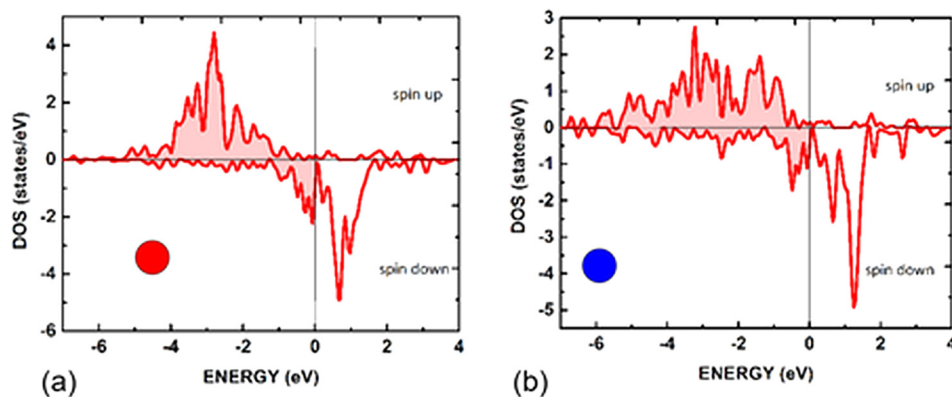


FIG. 4. Local DOS for the two nonequivalent Fe sites in Fig. 2: (a) site I (red) and (b) site II (blue).

catalysis-enhancing modification of the peak positions and heights. Note also that our focus is on the surface of the catalyst; no specific reactions are considered at this stage.

C. Local densities of states

Catalytic action occurs at specific sites on solid surfaces, usually called “active sites.” This means that the rate of catalytic reaction can be significantly increased by using very high surface area catalysts. It is important to keep in mind that $|\psi_{\mathbf{k}\nu}\rangle$ contains information from *all* atoms in the cluster or solid, and these all-atom features survive the projection procedure of Eq. (1).¹⁰ In other words, subsurface atoms are important in catalysis,¹⁴ but the corresponding hybridization effects are included in the present analysis.

The catalyst dispersion, defined as the number of surface atoms per total number of atoms, is usually larger than 0.01

and corresponds to catalyst particles ranging in size between 10 and 500 Å.¹ However, different surface sites behave differently from the viewpoint of catalytic activity. This catalytic activity strongly depends on the details of the catalytic reaction, but the local DOS plays an important role in distinguishing between different surface sites.

Figure 4 shows the local DOS for the two nonequivalent *iron sites* in the two Fe planes. The planes contain “blue” atoms forming a square in the center of the planes (II) and “red” outer atoms surrounding the square (I). Depending on the chemical reactions, the outer atoms (I) are more likely to be catalytically active, because they are easier to access by the reacting molecules. On the other hand, the DOS of the inner-square atoms (II) shows a larger number of well-separated peaks, which may be advantageous for some reactions. Note, however, that the peak positions relative to the Fermi level are as important as these steric considerations.

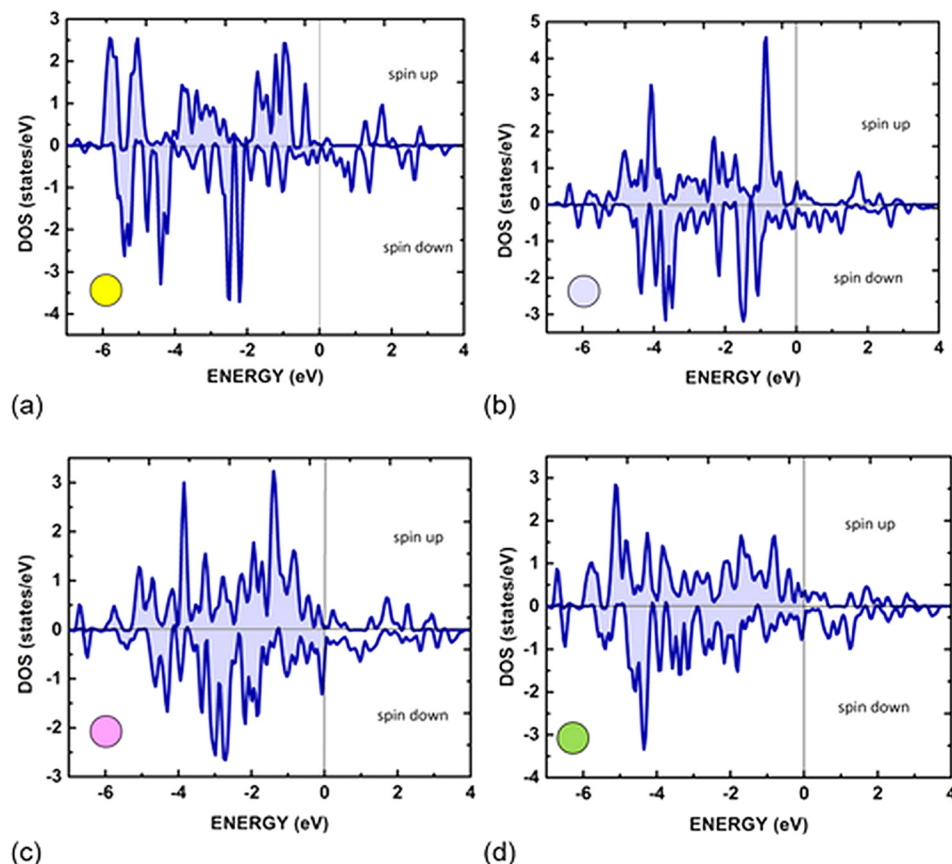


FIG. 5. Local DOS for the non-central nonequivalent Pt sites in Fig. 2: (a) site III (yellow), (b) site IV (light blue), (c) site V (magenta), and (d) site VI (green).

Figure 5 shows the local densities of states for the nonequivalent non-center atoms in the Pt planes. The "gray" center atom (VII) is surrounded by 8 atoms in the center plane, namely, 4 "magenta" corner atoms (V) and 4 "green" edge atoms (VI). The "yellow" (III) and "light blue" (IV) Pt forming the top and bottom planes of the clusters are clearly surface atoms and easily accessible by reacting molecules. The same is true for the corner atoms (V), whereas the edge atoms (VI) are located somewhat inside, similar to the "blue" (II) iron atoms. The local densities of states of all Pt sites (III–VII) exhibit a complicated peak structure and substantial exchange splitting. The former also occurs in nonmagnetic Pt nanoparticles, but the latter is limited to magnetic nanoparticles.

As we have seen in Sec. III A, the peak positions depend on the concentrations of the elements in the nanoparticle. Since catalytic reaction rates exhibit a strong dependence on the available energy levels, small stoichiometry changes may give rise to big changes in the catalytic performance. This freedom adds to the versatility created by having several nonequivalent sites. On the other hand, catalytic reactions also depend on the nature of the involved atomic orbitals. For example, the "light blue" Pt surface atom (IV) on the symmetry axis of the nanoparticle has both $5d |r^2\rangle$ and $5d |xy\rangle$ states. The $|r^2\rangle$ state is elongated along the symmetry axis and "sticks out" into the vacuum, enabling easy contact with reacting molecules. By contrast, the $|xy\rangle$ orbitals stay in the Pt planes, pointing towards the "yellow" (III) sites and likely being much less active.

From a practical viewpoint, finding the right magnetic nanoparticles for a given catalytic reaction is like looking for a needle in a haystack. Size, size distribution, chemical composition, atomic structure, and surface segregation in the presence of adsorbates all matter in the quest for maximizing the activity and concentration of active sites. However, preliminary experiments, such as Ref. 3, are encouraging, and the present work helps to clarify the opportunities and challenges in this research.

IV. CONCLUSIONS

In summary, we have analyzed how the relative contributions of 3d and 5d elements may affect the catalytic activity of magnetic catalysts, such as FePt alloys and nanoparticles. The DOS peaks do not simply change their magnitudes as a function of the concentration of 3d and 5d atoms, but also shift in energy, which should make it

possible to tune the catalytic activity. Furthermore, magnetic moment formation doubles the number of different levels that may potentially realize catalysis. The consideration of local densities of states makes it possible to distinguish between catalytically inert atoms inside the clusters and potentially active sites at the surface. Many of these surface DOS exhibit a complex structure with well-developed DOS peaks. Systematic variations of the composition and size of magnetic nanoclusters may therefore become a tool in the search for novel reaction-specific catalysts.

ACKNOWLEDGMENTS

This research was supported by NSF MRSEC (DMR-0820521), ARO (W911NF-10-2-0099), and NCMN-NRI. E.C.H.S. thanks the Division of Chemical Sciences, Office of Basic Energy Sciences, CPIMS Program, U.S. Department of Energy under Grant No. FG02-10ER16170.

- ¹N. D. Spencer and G. A. Somorjai, *Rep. Prog. Phys.* **46**, 1 (1983).
- ²V. A. Miransky and I. A. Shovkovy, *Phys. Rev. D* **66**, 045006 (2002).
- ³E. Kockrick, F. Schmidt, K. Gedrich, M. Rose, T. A. George, T. Freudenberg, R. Kraehnert, R. Skomski, D. J. Sellmyer, and S. Kaskel, *Chem. Mater.* **22**, 1624 (2010).
- ⁴A. Z. Moshfegh, *J. Phys. D: Appl. Phys.* **42**, 233001 (2009).
- ⁵B. Balamurugan, R. Skomski, and D. J. Sellmyer, in *Nanoparticles: Synthesis, Characterization and Applications*, edited by R. S. Chaughule and R. V. Ramanujan (American Scientific, Valencia, CA, 2010), p. 127.
- ⁶N. Toshima, Y. Shiraishi, A. Shiotsuki, D. Ikenaga, and Y. Wang, *Eur. Phys. J. D* **16**, 209 (2001).
- ⁷J. Govan and Y. K. Gun'ko, *Nanomaterials* **4**, 222 (2014).
- ⁸L. A. W. Green, T. T. Thuy, D. M. Mott, S. Maenosono, and N. T. K. Thanh, *RSC Adv.* **4**, 1039 (2014).
- ⁹M. Crosswhite, J. Hunt, T. Southworth, K. Serniak, A. Ferrari, and A. E. Stigman, *ACS Catal.* **3**, 1318 (2013).
- ¹⁰A. P. Sutton, *Electronic Structure of Materials* (University Press, Oxford, 1993).
- ¹¹J. K. Nørskov, *Rep. Prog. Phys.* **53**, 1253 (1990).
- ¹²A. U. Nilekar, K. Sasaki, C. A. Farberow, R. R. Adzic, and M. Mavrikakis, *J. Am. Chem. Soc.* **133**, 18574 (2011).
- ¹³M. D. Porosoff, W. Yu, and J. G. Chen, *J. Catal.* **308**, 2 (2013).
- ¹⁴T. H. Yu, T. Hofmann, Y. Sha, B. V. Merinov, D. J. Myers, C. Heske, and W. A. Goddard, *J. Phys. Chem. C* **117**, 26598 (2013).
- ¹⁵H.-L. Xin, A. Vojvodic, J. Voss, J. K. Nørskov, and F. Abild-Pedersen, *Phys. Rev. B* **89**, 115114 (2014).
- ¹⁶J. A. Chevary, S. H. Vosko, K. A. Jackson, M. R. Pederson, D. J. Singh, and C. Fiolhais, *Phys. Rev. B* **46**, 11 (1992).
- ¹⁷P. E. Blöchl, *Phys. Rev. B* **50**, 17953 (1994).
- ¹⁸N. I. Vlasova, G. S. Kandaurova, and N. N. Shchegoleva, *J. Magn. Magn. Mater.* **222**, 138 (2000).
- ¹⁹M. E. Gruner, G. Rollmann, P. Entel, and M. Farle, *Phys. Rev. Lett.* **100**, 087203 (2008).